European Journal of Cell Biology 91 (2012) 938–949

Contents lists available at SciVerse ScienceDirect

European Journal of Cell Biology

journal homepage: www.elsevier.com/locate/ejcb

Blood leukocytes and macrophages of various phenotypes have distinct abilities to form podosomes and to migrate in 3D environments

Céline Cougoule[a,b], Emeline Van Goethem[a,b], Véronique Le Cabec[a,b], Fanny Lafouresse[c,d,e], Loïc Dupré[c,d,e], Vikram Mehraj[f], Jean-Louis Mège[f], Claire Lastrucci[a,b], Isabelle Maridonneau-Parini[a,b,*]

[a] CNRS, IPBS (Institut de Pharmacologie et de Biologie Structurale), 205 route de Narbonne, BP 64182, F-31077 Toulouse, France
[b] Université de Toulouse, UPS, IPBS, F-31077 Toulouse, France
[c] INSERM, U1043, Toulouse, France
[d] CNRS, U5282, Toulouse, France
[e] Université de Toulouse, UPS, Centre de Physiopathologie de Toulouse Purpan, Toulouse, France
[f] Unité de Recherche sur les Maladies Infectieuses Tropicales et Emergentes, CNRS, UMR6236, Aix-Marseille Université, Marseille, France

ARTICLE INFO

Article history:
Received 6 March 2012
Received in revised form 18 July 2012
Accepted 19 July 2012

Keywords:
Migration
3D-environments
Podosomes
Macrophage polarization
T lymphocytes
Neutrophils
Monocytes
Inflammation

ABSTRACT

Leukocytes migrate through most tissues in the body, a process which takes place in 3D environments. We have previously shown that macrophages use the amoeboid migration mode in porous matrices such as fibrillar collagen I and the mesenchymal mode involving podosomes and matrix proteolysis in dense matrices such as Matrigel. Whether such a plasticity may apply to other leukocytes and to all subsets of macrophages is unknown. Here, we therefore provide a comparative analysis of the *in vitro* 3D migration modes adopted by primary human leukocytes. Blood-derived monocytes, neutrophils and T lymphocytes were found to use the amoeboid mode in a porous fibrillar collagen I matrix but were unable to infiltrate dense Matrigel and to form podosomes. M2-polarized macrophages and elicited peritoneal macrophages formed podosome rosettes, degraded the ECM and infiltrated both matrices. In contrast, M1 macrophages were motionless in 2D and 3D environments, whilst resident macrophages, devoid of podosomes, were only able to use the amoeboid mode. Thus, we conclude that whereas all leukocytes use the amoeboid mode to migrate through porous matrices, it is only certain macrophages that can adopt the mesenchymal mode that permits migration through dense matrices. Interestingly, the acquisition of mesenchymal migration capacity by macrophages correlates with the presence of podosomes and with their capacity to organize those as rosettes, which appears to be modulated by their differentiation and polarization states. As a perspective, specific control of the mesenchymal migration would be a potential target for therapeutic approaches aiming at decreasing macrophage tissue infiltration.

Introduction

Trafficking of leukocytes is a key process for immune cell development and host defence (reviewed in Friedl and Weigelin, 2008). Leukocytes are able to migrate through most tissues in the body and, *in vivo*, they encounter both 2-dimensional (2D) and 3-dimensional (3D) environments. 2D migration takes place along surfaces such as inner vessel walls and inner epithelial surfaces, whereas 3D migration takes place inside tissues composed of cells and extracellular matrix (ECM) protein scaffolds with heterogeneous composition and architecture.

We have shown that macrophages derived from blood monocytes (MDMs) can use either the amoeboid migration mode, a movement of rounded or ellipsoid cells that squeeze in and glide along the pores and gaps of a porous ECM, *e.g.* fibrillar collagen I (Friedl and Weigelin, 2008; Van Goethem et al., 2010) or the mesenchymal migration mode characterized by elongated cell morphology and requirement for proteases to progress in a non-porous environment such as Matrigel or gelled collagen I (Van Goethem et al., 2010). In environments with heterogeneous architecture, they combine the two migration modes (Guiet et al., 2011). From those studies, we concluded that the architecture of the matrix dictates the choice of the migration mode. Macrophages form podosomes constitutively in 2D environments (Linder, 2007).

* Corresponding author at: IPBS CNRS UMR5089, 205 route de Narbonne, BP 64182, F-31077 Toulouse, France. Tel.: +33 05 61 17 54 58; fax: +33 05 61 17 59 94.
E-mail address: isabelle.maridonneau-parini@ipbs.fr (I. Maridonneau-Parini).

0171-9335/$ – see front matter © 2012 Elsevier GmbH. All rights reserved.
http://dx.doi.org/10.1016/j.ejcb.2012.07.002

Podosomes are characterized as cell structures with proteolytic activity directed at the ECM, with a core of F-actin surrounded by a ring of adhesion receptors and actin-associated proteins such as vinculin and paxillin. In dense matrices, macrophages dig holes and form specialized F-actin rich structures called 3D podosomes at the tip of cell protrusions where proteolytic degradation of the matrix takes place (Van Goethem et al., 2010, 2011). We have previously proposed that podosomes are an essential requirement of the mesenchymal mode (Cougoule et al., 2010; Guiet et al., 2012), for the following reasons. First, 3D-podosomes are not formed in macrophages that use the amoeboid migration mode (Van Goethem et al., 2010). Second, Hck and Filamin A are two proteins involved in podosome stability, podosome organization as rosettes and ECM degradation, and both proteins are necessary for mesenchymal migration of macrophages but dispensable for amoeboid migration.

Macrophages can adopt the mesenchymal mode to infiltrate dense matrices (Van Goethem et al., 2010). The other leukocytes have been described to use the amoeboid migration mode (Friedl and Weigelin, 2008; Sabeh et al., 2009) but whether they can adopt the mesenchymal mode has not been investigated. Neutrophils have been described to use the amoeboid mode to infiltrate fibrillar collagen I (Sabeh et al., 2009) and podosome-related structures have been observed in murine neutrophils but the organization of vinculin as a ring and matrix proteolytic activity have not been documented to unequivocally characterize these structures (Calle et al., 2008; Szczur et al., 2006). T lymphocytes have been described to use the amoeboid migration mode in fibrillar collagen I (Wolf et al., 2003) and to also use podosome-related structures to palpate the surface of the endothelium to do transcellular diapedesis (Carman et al., 2007) and antigen recognition (Sage et al., 2012) but these structures have not been shown to have a proteolytic activity, a requisite to call them podosomes. Podosome structures have been largely characterized in monocyte-derived cells such as macrophages, osteoclasts and dendritic cells (Linder et al., 2011), but whether monocytes form podosome structures was never investigated. Thus, we investigated the ability of human blood-derived T lymphocytes, neutrophils and monocytes to migrate in a dense matrix in relation to their capacity to form podosome structures.

Macrophages exhibit various phenotypes as they polarize in response to environmental cues and can be broadly classified in two main groups: classically activated macrophages (or M1) and alternatively activated macrophages (or M2) (Delavary et al., 2011; Martinez et al., 2008, 2009; Mosser and Edwards, 2008; Murray and Wynn, 2011). Macrophages differentiate as M1 macrophages in response to IFN-γ and microbial products such as LPS. They typically take part in the initial immune response to invading microorganisms and promote T helper (Th) 1 immunity. M2 macrophages are obtained in response to IL4 or IL13 and are involved in the resolution phase of inflammation and tissue healing by promoting Th2 immunity (Delavary et al., 2011; Mege et al., 2011). Moreover, M2 macrophages have impaired phagocytosis capacity (Krysko et al., 2011; Varin et al., 2010). Because *in vitro* polarization of macrophages triggers phenotypes at the two extremes of a continuum of phenotypes which occur *in vivo*, we also studied the migration of macrophages collected from the peritoneal cavity in resting and acute inflammatory conditions was also studied.

For this study we thus set out to explore the 3D migration capacity of a variety of blood-derived leukocyte populations such as neutrophils, T lymphocytes and monocytes in porous (fibrillar collagen I) and dense (Matrigel) matrices polymerized *in vitro*. Since macrophages constitute a heterogeneous population *in vivo*, we also examined different macrophage subpopulations.

Materials and methods

Cell preparations

Blood samples from healthy donors were obtained following standard ethical procedures and with the approval of the concerned Internal Review Boards.

Human monocytes: Monocytes were isolated from blood (Etablissement Français du Sang, Toulouse, France) as previously described (Van Goethem et al., 2010). Those were then maintained in RPMI 1640 medium supplemented with 1% FCS and seeded on matrices polymerized in transwells (5×10^4) or ECM-coated coverslips (10^5).

Human neutrophils: Neutrophils were isolated from the same source by the dextran-Ficoll method as previously described (Le Cabec and Maridonneau-Parini, 1994). Cells were then maintained in RPMI 1640 supplemented with HEPES (10 mM), pH 7.4 for 20 min at 37 °C in suspension for recovery and layered down on matrices (5×10^4) or on ECM-coated coverslips (10^5). FCS at 1% final concentration was added after 1 h.

Human macrophages: Human macrophages derived from CD14-sorted monocytes (MDMs) were differentiated in the presence of M-CSF (20 ng/mL, Peprotech) as previously described (Van Goethem et al., 2010). After 7 days of differentiation, macrophages were polarized using either IFN-γ 20 ng/mL (100 U/mL-Roche) or IL4 (20 ng/mL-Miltenyi Biotec) for 18 h to obtain M1 and M2 polarized macrophages, respectively. TNFα (10 ng/mL) was also used to induce M1 polarization. All culture media contained M-CSF at 10 ng/mL during the polarization processes. MDMs had been serum starved for 4 h, harvested as previously described (Van Goethem et al., 2010), suspended in RPMI 1640 medium supplemented with 1% FCS, M-CSF (10 ng/mL) and the indicated cytokine and seeded on matrices (3×10^4) or ECM-coated coverslips (10^5).

Human lymphocytes: $CD4^+$ T cells were isolated by negative depletion using Rosette Sep (StemCell Technologies), cultured and expanded in RPMI 1640, 5% human serum, 100 U/mL IL2 in the presence of anti-CD3/CD28 coated Dynabeads (Invitrogen), with a bead:cell ratio of 1:1. Fresh IL2 was added every 3–4 days. $CD4^+$ T cells were restimulated as above every 19–21 days. When $CD4^+$ T cells were used, 14–21 days after activation, they were regaining a resting phenotype. Cell purity was assessed by FACS analysis (FACScan, Becton Dickinson) using PE-CY5-labelled anti-CD4 mAb (BD Biosciences) and was routinely between 95 and 99%. Cells were suspended in RPMI 1640 supplemented with 0.5% human serum and seeded on matrices (5×10^4) or ECM-coated coverslips (10^5).

Murine macrophages: Bone marrow-derived macrophages (BMDMs) from C57Bl6/J mice were obtained as previously described (Cougoule et al., 2010) and polarized using murine recombinant cytokines (ImmunoTools) according to the protocol described above for human macrophages. BMDMs had been serum starved for 4 h, harvested as previously described (Cougoule et al., 2010), suspended in RMPI 1640 supplemented with 1% FCS, 10 ng/mL M-CSF and the indicated cytokine, and seeded on matrices (5×10^4) or ECM-coated coverslips (10^5).

Tissue macrophages: C57Bl6/J mice were purchased from Charles River Inc. All experiments were performed with 6–12-week old female mice according to animal protocols approved by the Animal Care and Use committee of the Institut de Pharmacologie et de Biologie Structurale. Resident cells were collected by peritoneal lavages performed in control mice as previously described (Cougoule et al., 2010). Peritoneal elicited cells were collected 4 days after an intra-peritoneal injection of 0.5 mL of 4% thioglycollate Brewer (Sigma) as previously described (Cougoule et al., 2010). Collected cells were spun down (300 g) for 5 min, the pellet was suspended in RPMI 1640 medium and cells were layered down

on matrices (5×10^4) or ECM-coated coverslips (10^5). Medium was supplemented with 1% FCS after 1 h.

Matrix preparations

Collagen I (Nutragen – Nutacon; 2 mg/mL final concentration) or Matrigel (BD Biosciences, batches from 8 to 12 mg/mL) were polymerized as a thick layer (1–1.5 mm) in the upper Transwell chambers, as described (Van Goethem et al., 2010).

3D migration

Cells were seeded on the top of the matrices at the indicated concentration (see above). For all the cell types studied, the lower chambers were filled with RPMI 1640 medium supplemented with 10% FCS. For T lymphocytes and monocytes/macrophages, CXCL12 (1 μg/mL) and M-CSF (50 ng/mL) were added respectively. The percentage of 3D migration in fibrillar collagen I and in Matrigel was manually quantified after 24 h and 72 h, respectively using the ImageJ software.

2D migration

2D migration was performed in uncoated-8 μm porous transwells (BD Biosciences). Cells had been serum starved for 3 h. M1 or M2 polarized (3×10^4) MDMs were seeded in the upper chamber. The lower chamber was filled with 1 mL of RPMI 1640 supplemented with 10% of FCS and 50 ng/mL M-CSF. The migration assay was carried out overnight. The cells on the upper face were then removed using a cotton swab and the cells on the lower side were fixed with paraformaldehyde (3.7%; Sigma), permeabilized with Triton X-100 (0.1%; Sigma) and stained with Texas Red-coupled phalloidin (1/1000, Molecular Probes, Invitrogen) and DAPI [4,6-diamidino-2-phenylindole] (5 ng/mL, Sigma) to visualize F-actin and nuclei. The number of cells was then counted with a Leica DM-RB fluorescence microscope.

Matrix degradation assay

Coverslips were coated with 0.2 mg/mL FITC coupled-gelatin (Molecular Probes) as previously described (Cougoule et al., 2010). Macrophages or other leukocytes were cultured on FITC-coupled gelatin. For T lymphocytes, the gelatin-FITC had been coated with either fibronectin or ICAM-1 (10 μg/mL) for 1 h at 37 °C. After 24 h in culture, cells were fixed, processed for F-actin staining and observed by fluorescence microscopy. Quantification of the matrix degradation was assessed as previously described (Cougoule et al., 2010).

Immunofluorescence microscopy

BMDMs, murine tissue macrophages and other leukocytes had been cultured for 24 h on glass coverslips coated either with fibronectin, fibrinogen (10 μg/mL; Sigma) or nothing, or with ICAM-1 Fc chimera (10 μg/mL, R&D system) for T lymphocytes. Based on our previous data showing that macrophages spread on glass, coated or not with ECM proteins, spontaneously form podosomes after 15–30 min, we investigated podosome formation in blood-derived leukocytes at different time points starting from 60 min till 24 h. Cells were fixed with paraformaldehyde (3.7%; Sigma), permeabilized with Triton X-100 (0.1%; Sigma), and stained with anti-vinculin antibody (clone HVin-1, dilution 1/300; Sigma) followed by Alexa488-conjugated goat anti-mouse immunoglobulin G (1/1000; Cell Signalling Technology), Texas Red-coupled phalloidin and DAPI. Slides were visualized with a Leica DM-RB fluorescence microscope or with an LSM710 confocal microscope equipped with an x63-1.4 oil immersion Plan-Apochromat objective (CarlZeiss AG, Jena, Germany).

Table 1
Sequence primers used to characterize the M1 and M2 marker expression.

Primer	Sequence
Human markers	
hCXCL9-R	TCT-TTT-GGC-TGA-CCT-GTT-TCT-C
hCXCL9-L	AGT-GGT-GTT-CTT-TTC-CTC-TTG-G
hINDO-R	CAA-AAT-AGG-AGG-CAG-TTC-CAG-T
hINDO-L	TCA-TCT-CAC-AGA-CCA-CAA-GTC-A
hTNF-R	AGG-AGG-GGG-TAA-TAA-AGG-GAT-T
hTNF-L	CAT-CTA-TCT-GGG-AGG-GGT-CTT-C
hIL-15R	GTT-AGC-AGA-TAG-CCA-GCC-CAT-AC
hIL-15 L	TAC-TCA-AAG-CCA-CGG-TAA-ATC-C
hALOX15-R	GGG-GGC-TGA-AAT-AAC-CAA-AG
hALOX15-L	AAC-TTC-CAC-CAG-GCT-TCT-CTC
hCCL13-R	ATG-TGA-AGC-AGC-AAG-TAG-ATG-G
hCCL13-L	GAG-CAG-AGA-GGC-AAA-GAA-ACA
hDCSIGN-R	CAG-CAG-AGG-AAA-GAG-AGA-GAG-G
hDCSIGN-L	AGA-AGG-GTA-GGA-CTG-GAT-GTT-G
hFN1-R	CCA-CAG-AGT-AGA-CCA-CAC-CAC-T
hFN1-L	ACA-CCT-GGA-GCA-AGA-AGG-ATA-A
Murine markers	
mTNF-R	TCTGGAAAGGTCTGAAGGTAGGA
mTNF-L	AGAAACACAAGATGCTCGGACA
mCXCL10-R	CGT-CAT-TTT-CTG-CCT-CAT-CCT
mCXCL10-L	TCT-GCT-CAT-CAT-TCT-TTT-TCA-TCG
mIL12p40-R	GACACGCCTGAAGAAGATGAC
mIL12p40-L	GCCATTCCACATGTCACTGC
mMR-R	CATGAGGCTTCTCCTGCTTCTG
mMR-L (Mrc1	TTGCCGTCTGAACTGAGATGG
mYIM1/2-R	CCACTGAAGTCATCCATGTC
mYIM1/2-L	GGGCATACCTTTATCCTGAG
mArg2-R	TGGATCAAACCTTGCCTCTC
mArg2-L	GCCGATCAAATGTCTGTTCC

For each species, the M1 and M2 markers are presented in regular and italic case, respectively.

M1/M2 transcriptional profiles of macrophages

RNAs were extracted from MDMs, BMDMs, resident and elicited mouse macrophages using RNeasy Mini Kit (Qiagen) with a DNase I step to eliminate DNA contaminants, as recently described (Ben Amara et al., 2010). The quantity and the quality of RNA were assessed using Nanodrop (Thermo Science, Maurens-Scopont, France) and 2100 Bioanalyser (Agilent Technologies, Massy, France), respectively. Real-time quantitative RT-PCR (qRT-PCR) was carried out as recently described (Ben Amara et al., 2010). In brief, reverse transcription of 150 ng of RNA was performed with the MMLV-RT kit (Invitrogen). cDNA was obtained using oligo(dT) primers and M-MLV reverse transcriptase (Invitrogen) and qPCR experiments were performed using SYBR Green Fast Master Mix (Roche Diagnostics, Meylan, France) and a SmartCycler (Cepheid, Maurens-Scopont, France). The M1 and M2 genes were selected according to a previously published list of M1 and M2 genes (Martinez et al., 2006; Tantibhedhyangkul et al., 2011). The primers were designed using Primer3 (http://frodo.wi.mit.edu/primer3) (Table 1). Results were normalized using the housekeeping gene β-actin and are expressed as fold change (FC) = $2^{-\Delta\Delta Ct}$, where $\Delta\Delta Ct = (CtTarget - CtActin)_{assay} - (CtTarget - CtActin)_{control}$.

Podosome life time measurement

CD14-sorted human monocytes were seeded in 8-wells coverglass Labtek chambers (10^5 cells/wells) and differentiated in the presence of M-CSF (20 ng/mL). At day 3, cells were washed twice with PBS and transduced with a mCherry-Lifeact lentiviral vector to visualize F-actin structures. Briefly, the transduction was initiated by adding 200 μL/well of a mix of RPMI 1640 without FCS and the

lentiviral vector (10^6 effective viral particles for 10^6 macrophages). After 1h30, 400 μL of complete medium was added. At day 6, the culture medium was removed and MDMs were polarized as described above. After 24 h, cells were imaged using an inverted microscope (Leica DMIRB, Leica Microsystems) equipped with a motorized stage and an incubator chamber to maintain the temperature and CO_2 concentration constant. Images were acquired with the Metamorph software, every 20 s in one *z*-plane for 40 min, and on 10 separate fields per cell type. Quantification of podosome life-span was measured manually from two independent experiments, using the ImageJ software for podosomes appearing and disappearing during the time-course of the experiment and results were expressed as the mean ± SEM of 100 podosomes from 10 cells.

Statistics

All data in the text and figures are expressed as mean (±SEM) and unpaired *T*-test statistical analysis was carried out with the Prism 4.0 software. A *p* value of less than .05 was considered significant ($^*p < .05$, $^{**}p < .01$, $^{***}p < .001$).

Results

T lymphocytes, neutrophils and monocytes use the amoeboid but not the mesenchymal migration mode

To study the 3D migration ability of leukocytes, we used two different matrices with distinct architectures which were polymerized as thick layers (>1 mm) to create a 3D environment (Van Goethem et al., 2010). Fibrillar collagen I is a porous matrix into which macrophages and other leukocytes have been shown to use the amoeboid migration mode (Sabeh et al., 2009; Van Goethem et al., 2010; Wolf et al., 2003). Matrigel is purified from a mouse sarcoma which, when used at 10 mg/mL, forms a dense and poorly porous extracellular matrix. In Matrigel, MDMs and BMDMs have been shown to migrate using the protease-dependent mesenchymal mode (Cougoule et al., 2010; Van Goethem et al., 2010) whilst neutrophils have been shown not to migrate into it (Steadman et al., 1997).

T cell motility thought 3D matrices was induced by the chemokine CXCL12, a ligand for CXCR4. We mainly studied cultured primary human $CD4^+$ T cells. Those express CXCR4 homogeneously whilst freshly isolated T lymphocytes express heterogeneous CXCR4 levels (Bleul et al., 1997). T lymphocytes infiltrated fibrillar collagen I and exhibited a pear shape characteristic of the amoeboid migration mode (Fig. 1A and B, left panel, arrow) but they did not infiltrate Matrigel (Fig. 1A and B, right panel). Similarly, freshly isolated total T cells were unable to infiltrate Matrigel but migrated readily in fibrillar collagen matrices (data not shown). Next, the presence of podosomes was examined. To optimize cell spreading, a prerequisite for podosome formation, T lymphocytes were seeded on ICAM-I coated coverslips and treated or not with PMA for 24 h. Even under these conditions, no podosome structure could be observed in T lymphocytes. Some displayed actin dots, but those were not surrounded by vinculin, a hallmark of podosomes (Fig. 1C, inset a) and failed to degrade the gelatin-FITC covered with ICAM-1 (Fig. 1D) or fibronectin (data not shown). Treatment with PMA, although it increased cell spreading, still did not trigger proteolytic activity towards ECM (data not shown). Thus, despite our efforts to provide favourable conditions, we could not get T lymphocytes neither to form podosomes, nor to exhibit proteolytic activity on ECM nor to migrate into Matrigel.

Neutrophils freshly isolated from blood infiltrated fibrillar collagen I (Fig. 1A and B) with a rounded cell shape but did not infiltrate Matrigel (Fig. 1A and B). Occasionally, a few F-actin dots with almost a regular ring of vinculin were noticed (Fig. 1C, inset b), but on glass, on fibronectin or vitronectin, neutrophils generally failed to form podosomes (Fig. 1C, inset a), and failed to degrade the matrix of FITC-gelatin (Fig. 1D). As the diapedesis step could be critical "to switch" cells to a competent migration phenotype in dense matrices, we then tested the migration ability of inflammatory neutrophils harvested from the mouse peritoneal cavity 12 h after injection of thioglycollate. At this time point, neutrophils accounted for 77.4 ± 4.7% ($n = 5$) of the collected cells (Fig. S1). Despite the inflammatory context from which they were obtained, elicited neutrophils still did not infiltrate Matrigel and did not form podosomes (data not shown).

Similarly, freshly isolated monocytes infiltrated the matrix of fibrillar collagen I with the typical amoeboid rounded cell shape (Fig. 1A and B) but not Matrigel (Fig. 1A and B). They formed F-actin dots which were not surrounded by vinculin and thus were not considered as podosomes (Fig. 1C). After 4–5 days on Matrigel, some monocytes did acquire the capacity to infiltrate the matrix with the characteristic elongated cell shape (Fig. 1B). At day 6, the percentage of cells into the matrix was quantified (Fig. 1A) and was similar to that previously described for macrophages after 7 days of differentiation in culture dishes (Van Goethem et al., 2010), suggesting that differentiation is required to infiltrate dense matrices.

Thus, none of the leukocytes studied here were found to have the capacity to infiltrate Matrigel or to form podosomes, suggesting that these cells are unable to use the protease-dependent mesenchymal mode.

In vitro polarized M1 or M2 human and mouse macrophages display distinct 3D migration abilities

Next, we investigated whether the 3D migration ability of monocyte-derived macrophages (MDMs) was regulated during macrophage polarization.

Human M1 and M2 MDMs were generated by IFN-γ- and IL4-treatment, respectively. Using a combination of 8 polarization markers, we checked that IFN-γ- and IL4-stimulated macrophages exhibited typical M1 and M2 profiles when compared to non-polarized MDMs that we called here M0 (Fig. 2A).

The migration ability of M1 and M2-polarized MDMs was examined in comparison with M0. M2 MDMs were able to migrate into fibrillar collagen I and Matrigel (Fig. 2B) with the typical cell shape of amoeboid and mesenchymal migration, respectively (Fig. 2C). They exhibited comparable migration ability than M0 macrophages (Fig. 2B and C). In marked contrast, IFN-γ-polarized M1 MDMs were unable to migrate into fibrillar collagen I or in Matrigel (Fig. 2B), and stayed at the top of the matrices where they displayed a rounded cell shape (Fig. 2C). To ensure that inhibition of the migration was the result of M1 polarization, MDMs were also polarized using TNFα (Mantovani et al., 2004). TNFα-treated MDMs did not migrate in fibrillar collagen I or in Matrigel (data not shown) confirming that M1 macrophages are defective in both migration modes.

To test the 2D migration ability of M1 and M2 macrophages, a standard transwell assay was used. As shown in Fig. 2D, M1 MDMs were also motionless in those conditions, while M2 were migrating even more efficiently than M0 macrophages. Taken together, these results show that M1 MDMs were defective for both 3D and 2D migration whereas M2 MDMs remained competent for all types of migration: 2D and 3D migration into fibrillar collagen I and Matrigel. The presence of podosomes was examined in M1 and M2 MDMs layered on fibrinogen. Individual podosomes were observed in 100% of the M1 and M2 macrophages. Live observations of mCherry-Lifeact-expressing M1 and M2 MDMs revealed that the lifetime of individual podosomes in M1 MDMs was 625 ± 59 s while it was 411 ± 42 s in M2 macrophages ($p = 0.0037$, $n = 100$ podosomes/condition) (to compare with podosomes in

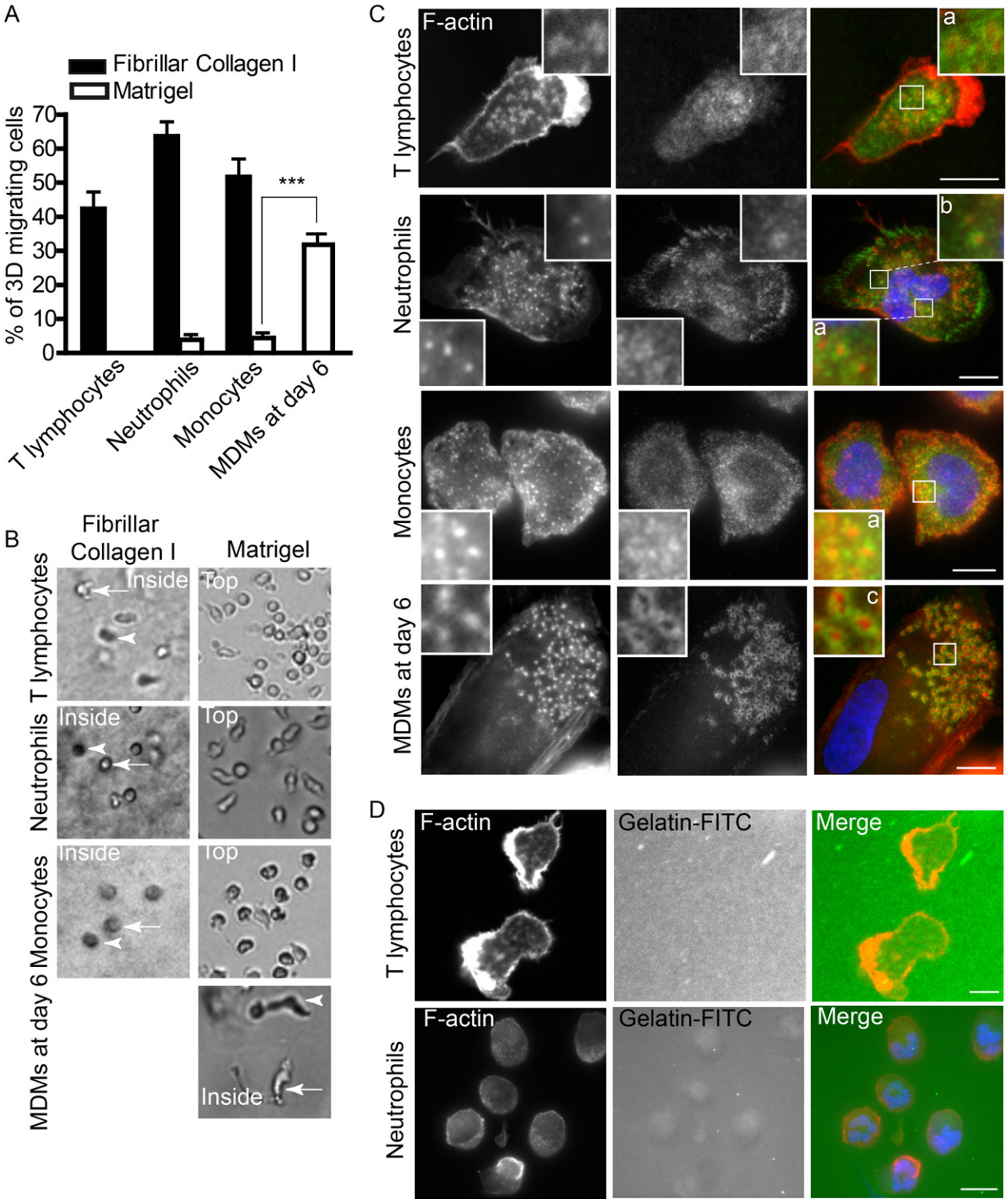

Fig. 1. T lymphocytes, neutrophils and monocytes only use the amoeboid migration mode. (A) Cells were seeded at the top of a thick layer of fibrillar collagen I or Matrigel and the 3D cell migration was quantified after 24 h and 72 h, respectively. T lymphocytes, neutrophils and monocytes infiltrated the matrix of fibrillar collagen I but did not infiltrate Matrigel. After 6 days on the matrix, monocyte-derived macrophages (MDMs) which had acquired the capacity to infiltrate Matrigel were quantified as described in the section "Materials and methods". Results are expressed as mean ± SEM of three independent experiments performed in triplicates, $^{***}p < 0.001$. (B) T lymphocytes, neutrophils and monocytes migrating either inside fibrillar collagen I (left panels, arrows) or on top of the Matrigel matrix (right panels, arrows) are shown. Arrowheads show cells at a distinct depth in the matrices. (C) T lymphocytes were seeded on ICAM-I coated coverslips (without PMA treatment) for 24 h, neutrophils were seeded on glass coverslips for 1 h, monocytes and macrophages were seeded on glass coverslips for 24 h. All cells were fixed and permeabilized. F-actin was stained with Texas Red-coupled phalloidin, vinculin was stained with primary and AlexaFluor 488-coupled secondary antibodies, and nuclei with DAPI. T lymphocytes, neutrophils and monocytes formed F-actin dots but vinculin did not form a ring around the actin core (insets (a)). Inset (b) illustrates the presence of few F-actin dots with a quite regular ring of vinculin in neutrophils. Inset (c) illustrates the organization of classical podosomes with a ring of vinculin in MDMs after 6 days of culture. Scale bars: 10 μm, insets = 3× magnification. (D) T lymphocytes and neutrophils seeded on FITC-coupled gelatin coated on glass coverslips and cultured either overnight or for 5 h, respectively, were fixed and stained for F-actin and nuclei and microscopically examined. Neither T lymphocytes nor neutrophils degraded FITC-coupled gelatin. Scale bars: 10 μm.

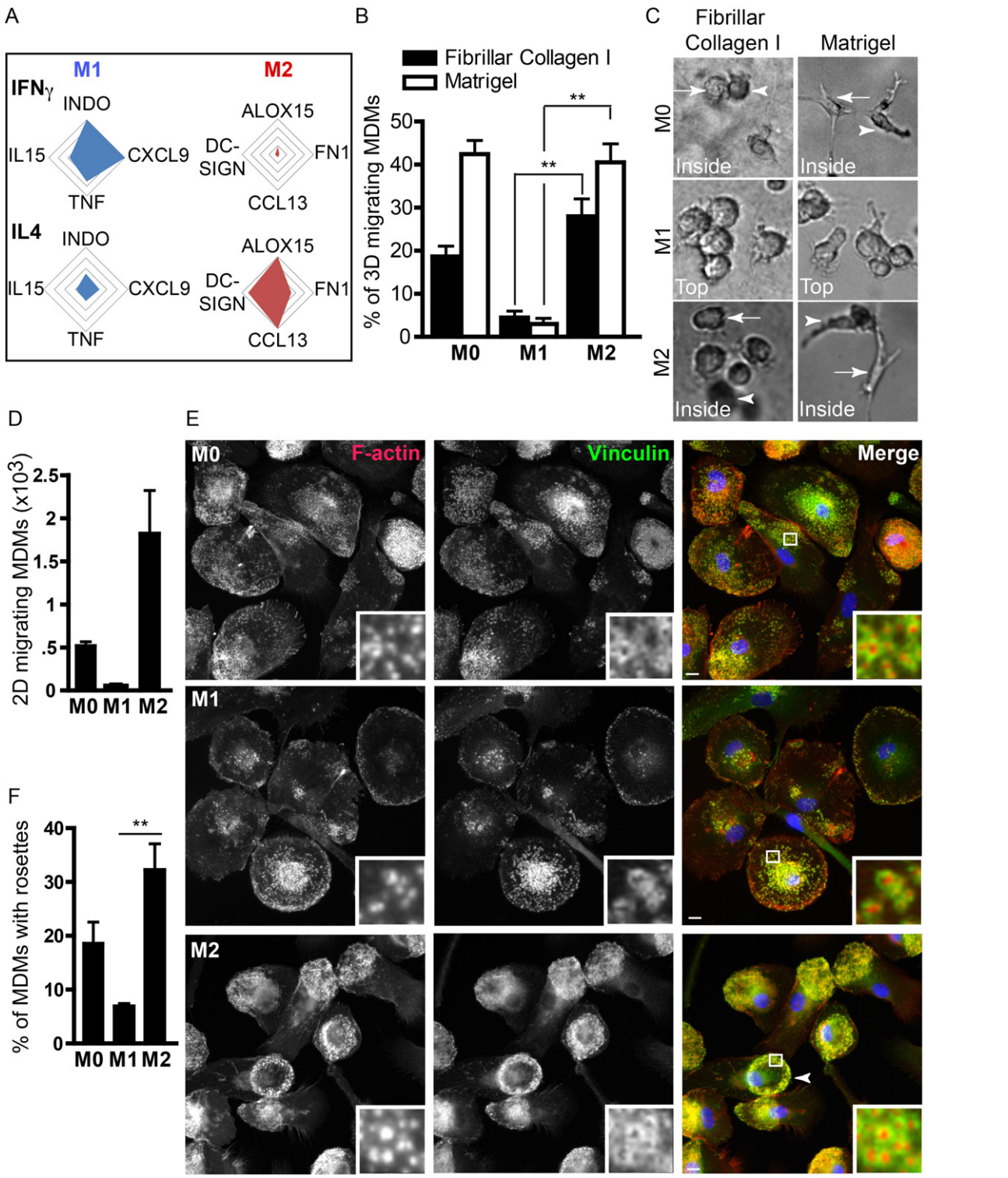

Fig. 2. M2 but not M1 human macrophages migrate in 3D matrices. MDMs were stimulated with nothing (M0), IFN-γ or IL4 to induce M1 and M2 polarization respectively. (A) Total mRNA was extracted and the expression of 4 M1-related genes (IL15, INDO, TNF, CXCL9) and M2-related genes (DC-SIGN, ALOX15, CCL13, FN1) was measured by real time RT-PCR. Results are expressed as fold change (FC) compared to M0 macrophages and represent the mean of three experiments. They are presented as radar plots with a maximum increase of 4 folds. (B) M0, M1 and M2 MDMs were harvested and seeded on top of a thick layer of fibrillar collagen I or Matrigel and cell migration was quantified from triplicate samples after 24 h and 72 h, respectively. Results are expressed as mean ± SEM of four independent experiments, $^{**}p < 0.01$. (C) M0 and M2 MDMs are shown inside fibrillar collagen I or in Matrigel while M1 macrophages which mostly do not infiltrate matrices are shown at the top. Arrowheads show cells deeper in the matrices. (D) 2D migration of M0, M1 and M2 MDMs through uncoated transwells. MDMs that reached the lower chamber were microscopically counted. Results are expressed as mean ± SEM of two independent experiments. (E) M0, M1 and M2 MDMs were seeded on fibrinogen-coated glass coverslips for 24 h, fixed, permeabilized and F-actin was stained with Texas Red-coupled phalloidin, vinculin with primary and AlexaFluor 488-coupled secondary antibodies, and nuclei with DAPI. M1 MDMs harbor individual podosomes (inset) while M2 MDMs harbor podosome rosettes (arrowhead and inset). Scale bar = 10 μm, insets = 6× magnification. (F) Quantification of podosome rosettes in M0, M1 and M2 MDMs. Podosome structures were counted in at least 100 cells in duplicate samples, in three separate experiments. $^{**}p < 0.01$.

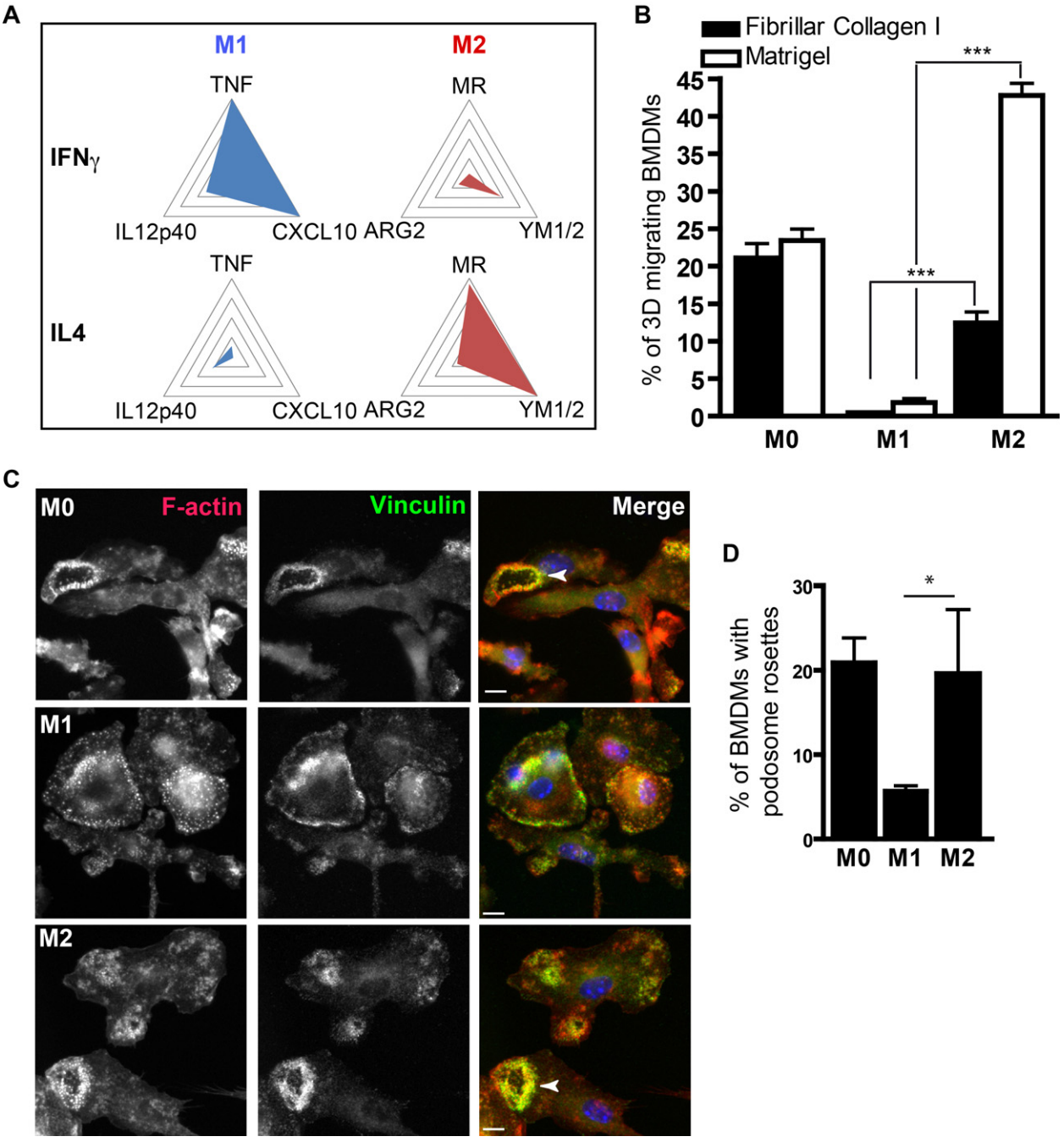

Fig. 3. M2 but not M1 mouse macrophages migrate in 3D matrices. Mouse bone marrow-derived macrophages (BMDMs) were stimulated with nothing, IFN-γ or IL4 to induce M0, M1 and M2 polarization, respectively. (A) Total mRNA was extracted and the expression of 3 M1-related genes (TNFα, CXCL10, IL12p40) and M2-related genes (Manose Receptor (MR), YM1/2, Arginase 2 (ARG2)) was measured by real time RT-PCR. The results are expressed as fold change compared to M0 BMDMs and represent the mean of three experiments. They are presented as radar plots with a maximum increase of 4 folds. (B) M0, M1 and M2 BMDMs were harvested and seeded on top of a thick layer of fibrillar collagen I or Matrigel and the 3D cell migration was quantified after 24 h and 72 h respectively from triplicate samples. Results are expressed as mean ± SEM of three independent experiments, $^{***}p < 0.001$. (C) M0, M1 and M2 BMDMs were seeded on fibronectin-coated glass coverslips for 24 h, fixed, permeabilized and F-actin was stained with Texas Red-coupled phalloidin, vinculin with primary and AlexaFluor 488-coupled secondary antibodies, and nuclei with DAPI. M1 BMDMs form few podosome rosettes while M0 and M2 BMDMs harbor podosome rosettes (arrowheads). Scale bar = 10 μm. (D) Quantification of podosome rosettes in M0, M1 and M2 BMDMs. Podosome structures were counted in at least 100 cells in duplicate samples, in three independent experiments. $^{*}p < 0.05$.

M0 macrophages which is approximately 400 s (Bhuwania et al., 2012)). These results indicate that M1 macrophages have a reduced podosome turnover compared to M2 . In murine bone marrow derived macrophages (BMDMs), we have previously reported that the organization of podosomes as rosettes is required for mesenchymal migration (Cougoule et al., 2010). Thus, we quantified podosome rosettes in M0, M1 and M2 MDMs layered on fibrinogen. As shown in Fig. 2E and F, similarly to M0, M2 MDMs efficiently organized their podosomes as clusters and rosettes while M1 MDMs hardly formed these structures. The presence of rosettes has been correlated with enhanced ECM proteolytic activity (Cougoule et al., 2010) but somewhat surprisingly, M1 MDMs were found to degrade gelatin-FITC with the same efficiency as M0 and M2 cells (Fig. 4C). One noticeable difference, however, was that M1 MDMs harbored a "sitting" cell shape on gelatin-FITC with a large degradation area under the cells, whereas M2 MDMs harbored a

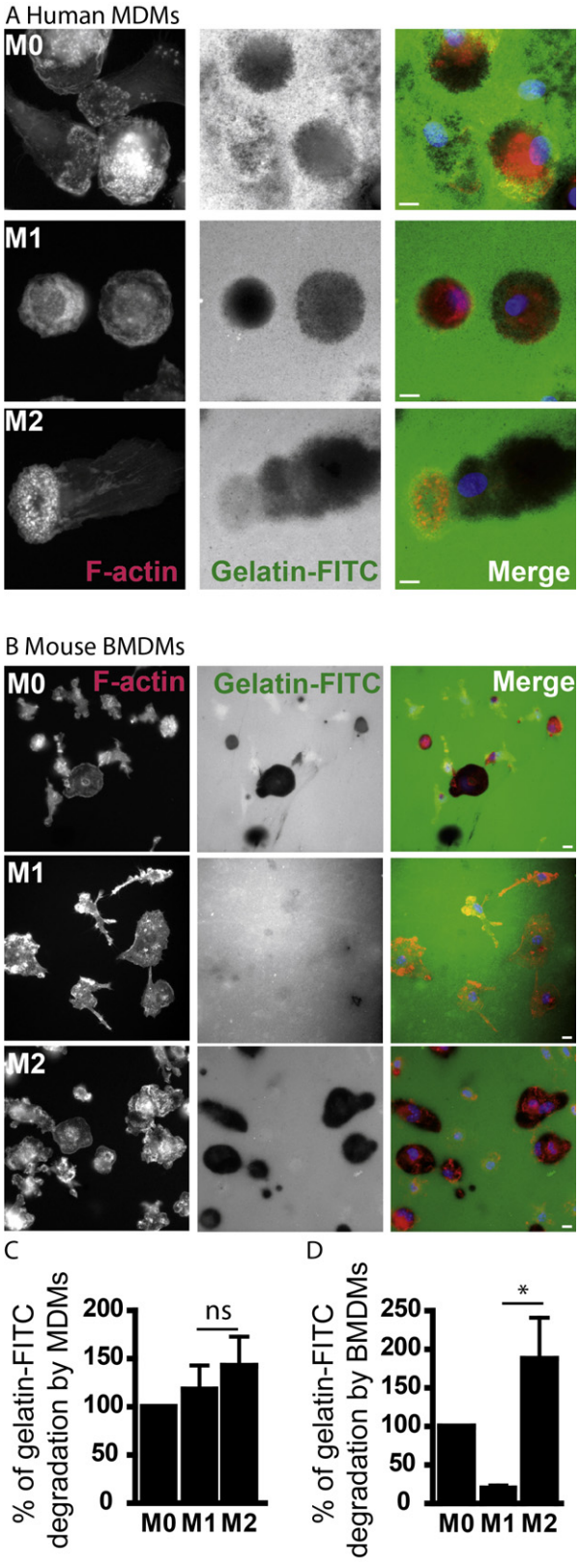

Fig. 4. (A) M0, M1 and M2 MDMs were seeded on FITC-coupled gelatin coated on glass coverslips, cultured overnight, fixed and stained for F-actin and nuclei and microscopically examined. Scale bar: 10 μm. (B) M1 BMDMs are defective in gelatin-FITC degradation. M0, M1 and M2 BMDMs were seeded on FITC-coupled gelatin coated on glass coverslips and incubated overnight, fixed and stained for F-actin and nuclei. Scale bar: 10 μm. (C) Quantification of gelatin-FITC degradation by M0, M1 and M2 MDMs. The percentage of degradation corresponds to the number of pixels of degradation for 100 pixels of cell surface. Results are expressed as mean ± SEM ($n = 3$). (D) Quantification of the percentage of gelatin-FITC degradation by M0, M1 and M2 BMDMs. The percentage of degradation corresponds to the number of pixels of degradation for 100 pixels of cell surface. Results are expressed as mean ± SEM ($n = 3$), $^*p < 0.05$.

"migrating" phenotype characterized by a polarized shape with podosomes or podosome rosettes localized at the leading edge (Fig. 4A). Thus the proteolytic activity of M1 macrophages which form more stable podosomes appeared to be similar to M2 cells which form podosome rosettes and are motile.

Differences have been described between human and murine polarized macrophages (Martinez et al., 2006). We thus investigated the migration capacity of polarized mouse macrophages derived from bone marrow (BMDMs). Those were polarized in M1 and M2 BMDMs, as controlled by analysis of the expression of six polarization markers (Fig. 3A). Similarly to human macrophages, M1 BMDMs did not migrate into fibrillar collagen I or Matrigel while M2 BMDMs did and even better than M0 macrophages in Matrigel (Fig. 3B). In addition, 100% of mouse M1 and M2 macrophages formed individual podosomes when layered on fibronectin but only M2 BMDMs organized their podosomes as rosettes (Fig. 3C and D). The only difference between human and mouse cells we observed in our experiments was that mouse M1 BMDMs showed relatively low gelatin-FITC degradation capacity (Fig. 4B and D). Taken together, these results indicate that the M1 polarization process is characterized by a motionless phenotype, the inability to organize podosomes as rosettes and an heterogeneous capacity to degrade the matrix, while M2 polarized cells are able to migrate effectively in both matrices, form rosettes and degrade the matrix.

The migration ability of elicited macrophages differs from that of resident macrophages

We next examined the ability of resident and elicited macrophages harvested from the mouse peritoneal cavity to migrate in 3D matrices, to form podosome structures and degrade gelatin-FITC. Elicited macrophages were collected 4 days after intraperitoneal injection of thioglycollate.

We compared the expression of 6 biomarkers between elicited and resident macrophages to characterize their polarization profiles. As shown in Fig. 5A , elicited macrophages displayed a combined expression of the M1 and M2 markers.

While both cell types migrated in fibrillar collagen I, only elicited macrophages migrated in Matrigel (Fig. 5B and C), formed podosome rosettes (Fig. 5D and E) and degraded the gelatin-FITC matrix (Fig. 5F and G).

Thus resident and elicited macrophages which are known to exert distinct functionalities (Gordon and Mantovani, 2011) exhibit distinct migration behavior, providing further information about the phenotypic heterogeneity of tissue macrophages.

Discussion

The data presented herein extend our knowledge of the 3D migration ability of several leukocyte populations into thick extracellular matrices. We observe that (i) circulating leukocytes use the amoeboid mode, do not form podosomes and are unable to infiltrate dense matrices and (ii) the migration of macrophages, which have been previously shown to use the amoeboid and the mesenchymal mode in porous and dense matrices, respectively, is strongly influenced by polarization and the tissue environment.

3D migration takes place when leukocytes enter interstitial tissues beyond vessels and the basal membrane. The architecture of interstitial tissues is heterogeneous, ranging from loose fibrillar regions to dense compact connective tissue with submicron

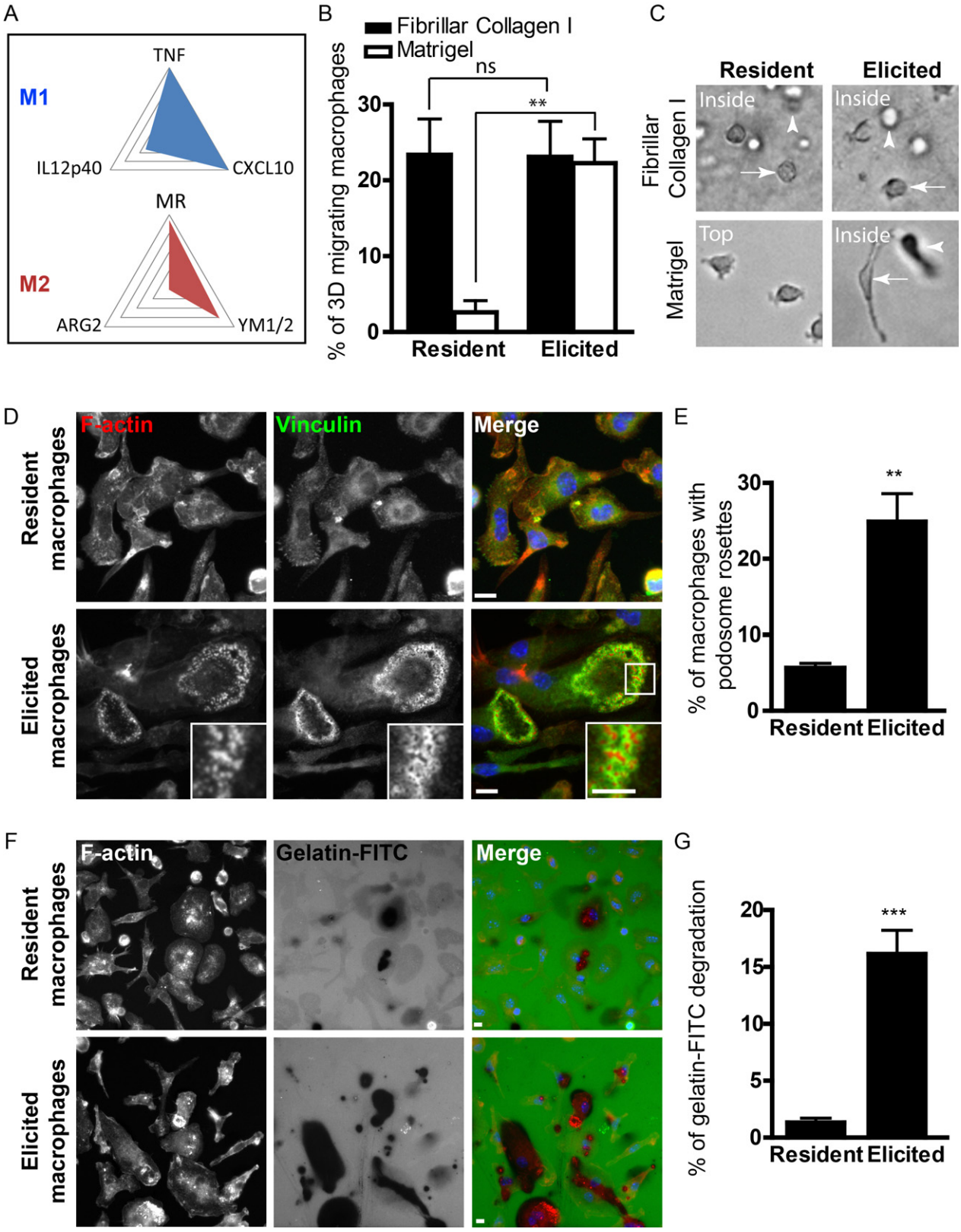

Fig. 5. Elicited but not resident macrophages use the mesenchymal migration mode. Resident and elicited macrophages were harvested from mouse peritoneal cavity. Elicited macrophages were collected 4 days after an intraperitoneal injection of thioglycollate. (A) Total mRNA was extracted from resident and elicited macrophages and the expression of 3 M1 related genes (TNF, CXCL10, IL12p40) and 3 M2 related genes (MR, YM1/2, ARG2) was measured by real time RT-PCR. The results are expressed as FC of elicited on resident macrophages and represent the mean of 3 experiments. They are presented as radar plots with a maximum increase of 4 folds. (B) Resident and elicited macrophages were harvested and seeded on top of a thick layer of fibrillar collagen I or Matrigel and 3D cell migration was quantified after 24 h and 72 h respectively from triplicate samples. Results are expressed as mean ± SEM of five independent experiments, $^{***}p < 0.001$. (C) Resident macrophages migrating inside fibrillar collagen I (arrow) or on top of Matrigel are shown. Elicited macrophages migrating inside fibrillar collagen I or Matrigel are shown (arrow). Arrowheads show cells at a different depth in matrices. (D) Tissue macrophages were seeded on fibronectin-coated glass coverslips for 24 h, fixed, permeabilized and F-actin was stained with Texas Red-coupled

spacing (Egeblad et al., 2010; Larsen et al., 2006). Thus two matrices which have been described in detail in a previous report (Van Goethem et al., 2010) were used to mimic the architectural heterogeneity of interstitial tissues. In fibrillar collagen I, neutrophils, T lymphocytes and human macrophages have been described to use the amoeboid migration mode (Nourshargh et al., 2010; Sabeh et al., 2009; Van Goethem et al., 2010; Wolf et al., 2003). Herein, we compared, in the same experiments, the migration capacity of leukocytes in porous fibrillar collagen I and in a dense Matrigel. We confirm the ability of monocytes, neutrophils and T lymphocytes to migrate using the amoeboid mode in fibrillar collagen I, and we show that they do not infiltrate Matrigel. Using the experimental conditions which trigger the formation of podosomes in macrophages, dendritic cells and osteoclasts (Linder et al., 2011), namely on glass coated or not with ECM proteins, we observed that T lymphocytes, neutrophils and monocytes do not form podosomes, according to the definition of these cell structures which implicates an actin dot surrounded by a ring of vinculin and a proteolytic activity towards the ECM (Linder et al., 2011). It has been reported that T lymphocytes form podosome-like structures during trans-cellular migration through the endothelium (Carman et al., 2007) and scanning for antigen on antigen presenting cells (Sage et al., 2012). In those experiments, however, the proteolytic activity of those structures was not established, a requisite for qualifying these structures as podosomes.

That neutrophils, monocytes and T lymphocytes are unable to infiltrate Matrigel is surprising as these cells are expected to migrate in most tissues. One hypothesis is that steps of differentiation might be missing. For our experiments, we have used cells isolated from blood which were then differentiated *in vitro*. Thus, compared to the *in vivo* context, diapedesis is by-passed and this step could be critical "to switch" cells to a competent migration phenotype in dense matrices. Using elicited neutrophils which had accomplished this step of diapedesis, however, we found that those cells still did not form podosomes, nor did T lymphocytes differentiated with anti-CD3/CD28 Abs in the presence of IL2 for 2–3 weeks acquire the capacity to migrate in Matrigel. Since neutrophils and lymphocytes are small cells which might glide into small pores (Van Goethem et al., 2011), another hypothesis is that leukocytes unable to use the mesenchymal mode would only infiltrate loose areas in tissues. In agreement with this proposal, a recent report on lung tumor biopsies shows that T lymphocytes are unable to cross dense fibers of ECM proteins surrounding tumor islets and remain in regions of loose tissue (Salmon et al., 2012). It should be noted that neutrophils have a segmented nucleus which might facilitate infiltration into poorly porous tissues. In fact, a recent report shows that in tumor microenvironments, the nuclei of infiltrated neutrophils are even more segmented than control neutrophils (Fridlender et al., 2009), suggesting that, by modifying their nuclear morphology, neutrophils could more easily squeeze in poorly porous tissues such as tumors (Egeblad et al., 2010) using the amoeboid migration. In the case of migration into the dense Matrigel matrix, used in our experiments at approximately 10 mg/mL, the size of the pores is apparently too narrow (see a scanning electron microscopy picture of the architecture of Matrigel in Van Goethem et al. (2010)) to allow neutrophil migration. A previous report has shown that neutrophils can infiltrate Matrigel in a protease-independent manner when it is diluted to 3 mg/mL (Steadman et al., 1997) indicating that a lower density allows neutrophils to infiltrate Matrigel using the amoeboid mode.

In conclusion, these three types of leukocytes are unable to migrate in matrices which require the formation of paths in a protease-dependent manner, while they migrate in porous 3D environments using the amoeboid mode. Thus, if the same rules apply *in vivo*, we would expect to find these cells only in porous tissue areas.

In marked contrast, when monocytes (from human blood) differentiate in macrophages, they become able to infiltrate Matrigel using the mesenchymal migration mode (Van Goethem et al., 2010, this report). Similar observations have been made with mouse macrophages differentiated from bone marrow (Cougoule et al., 2010). Because macrophages have a large plasticity, we examined the migration of polarized and of tissue macrophages to get further insight into their respective 3D migration abilities. Macrophages polarized as M1 or M2 exhibit distinct functions. M1 macrophages are involved in the early phase of the inflammatory response (Bystrom et al., 2008; Mege et al., 2011), they release inflammatory mediators and bactericidal products and they actively ingest microorganisms and cellular debris (Liddiard et al., 2011). We report that M1 macrophages do not migrate in 2D and 3D environments. Despite the fact that distinct molecular mechanisms govern 2D and 3D migration (Harunaga and Yamada, 2011), these results suggest that a common step may be inactivated. The observation that macrophages become motionless under inflammatory processes is important as it might contribute to maintain macrophages at the site of infection to clean out bacteria and release toxic bactericidal products only in limited tissue areas (Laskin et al., 2011). M1 BMDMs have been shown to adhere to extracellular matrices to a higher extent than M2 (Vereyken et al., 2011) and, in the same line, we report that podosomes in M1 cells are more stable than in M2 macrophages. M2 macrophages have been characterized as anti-inflammatory cells with healing properties to curtail inflammation after an infection or an injury and promote to return the body to homeostasis (Delavary et al., 2011; Serhan and Savill, 2005). It has been reported that mouse M2 BMDMs have a higher 2D motility towards conditioned medium than their M1 counterpart (Vereyken et al., 2011). Similar results were obtained here with human M2 MDMs, and we showed further that mouse and human M2 macrophages can migrate in both fibrillar collagen I and Matrigel, and form podosomes that they organize as rosettes. Interestingly, M2 polarization induces an increase in fibronectin transcript which is involved in cell adhesion and migration processes and in cathepsin C, a lysosomal protease which could be involved in mesenchymal migration (Martinez et al., 2006; Verollet et al., 2011). Moreover, Hck, which regulates the formation of podosome rosettes and the protease-dependent 3D migration of macrophages (Cougoule et al., 2010), is activated during the process of M2-polarization (Bhattacharjee et al., 2011). M2 macrophages are also associated with pathological contexts such as persistent infections (tuberculosis, leprosy, Whipple's disease (Mege et al., 2011). In the light of our results, it would be interesting to examine whether M2 macrophages facilitate host dissemination of pathogens. M2 macrophages are also described in chronic autoimmunity, obesity, fibrosis and cancer (Fairweather and Cihakova, 2009; Gordon and Martinez, 2010; Mosser and Edwards, 2008; Sica and Mantovani, 2012)). In several tumor models, macrophages have

phalloidin, vinculin with primary and AlexaFluor 488-coupled secondary antibodies, and nuclei with DAPI. Elicited macrophages organized their podosomes as rosettes (insets). Scale bars: 10 μm, inset = 3× magnification. (E) Quantification of podosome rosettes in resident and elicited macrophages. Podosome structures were counted in at least 100 cells in duplicate samples ($n = 5$), $^{**}p < 0.01$. (F) Resident and elicited macrophages were seeded on FITC-coupled gelatin coated on glass coverslips and incubated overnight, fixed and stained for F-actin and nuclei. Resident macrophages poorly degrade FITC-coupled gelatin. Elicited macrophages degraded large areas of gelatin-FITC. Scale bars: 10 μm. (G) Quantification of FITC-coupled gelatin degradation by resident and elicited macrophages. The percentage of degradation corresponds to the number of pixels of degradation for 100 pixels of cell surface. Results are expressed as mean ± SEM ($n = 5$), $^{***}p < 0.001$.

been shown to be polarized as M2 and to enhance malignancy and tumor cell invasiveness (Qian and Pollard, 2010; Ruffell et al., 2012) notably by remodeling the extracellular matrix to open paths to tumor cells (Gocheva et al., 2010; Guiet et al., 2011).

Despite the fact that *in vitro* polarization is clearly a simplified model, results on cell migration provide new striking differences between M1 and M2 macrophages, namely that 2D and 3D migration is an exclusive property of M2 macrophages.

We also report that resident and elicited peritoneal macrophages have distinct migration abilities. Elicited peritoneal macrophages, harvested 4 days after thioglycollate injection, were found to up-regulate both M1 and M2 markers as previously reported (Schif-Zuck et al., 2011; Stables et al., 2011) and to migrate in both fibrillar collagen I and Matrigel. At this time point, the inflammatory response initiated by thioglycollate is reaching the resolution phase (C. Lastrucci et al., unpublished data) and macrophages are thus not expected to die locally but to migrate to the draining lymph nodes (Bellingan et al., 1996; Randolph, 2008). For this, motile functions in 3D environments would be necessary.

Resident macrophages originate either from blood monocytes which migrate to tissues in non-inflammatory conditions or from resident cells which self-renew by transient proliferation after inflammatory episodes (Davies et al., 2011; Jenkins et al., 2011). One of the functions of resident macrophages is to sample the tissue in search of foreign particles. We show that peritoneal resident macrophages migrate in fibrillar collagen I but not in Matrigel. As previously described (Isaac et al., 2010), we observed that resident macrophages do not form podosome rosettes and they do not degrade gelatin-FITC. Consequently, in contrast to elicited macrophages, residents have a limited migration ability which might confine them to their tissue of residence. In future, it will be interesting to explore whether resident macrophages collected from tissues with distinct biophysical properties (porosity, stiffness) have distinct migration abilities compared to peritoneal macrophages.

We have previously shown that migration of human and mouse macrophages in dense matrices such as Matrigel or gelled collagen I is: (i) inhibited by protease inhibitors, (ii) independent of ROCK, a key effector of the amoeboid migration, (iii) dependent on the macrophage ability to organize its podosomes as rosettes and to degrade the ECM, (iv) characterized by an elongated cell shape with 3D podosomes at the tip of cell protrusions (Van Goethem et al., 2010, 2011; Verollet et al., 2011). This mode of migration has been called mesenchymal migration (Cougoule et al., 2010; Van Goethem et al., 2010, 2011; Verollet et al., 2011) by analogy to a migration mode used by tumor cells (Wolf and Friedl, 2011). Taken together with our previous studies, we show that cells which are able to infiltrate Matrigel with the characteristic mesenchymal phenotype (MDMs, BMDMs, human and mouse M2 macrophages, mouse elicited macrophages) form podosomes, organize them as rosettes and degrade the ECM while cells which do not infiltrate Matrigel (T lymphocytes, neutrophils, monocytes and resident macrophages) do not form podosomes. Although podosomes are required for the mesenchymal mode, the presence of podosomes does not certify the mesenchymal migration ability since M1 MDMs do form podosomes and degrade the matrix but are motionless. Interestingly, M1 macrophages do not organize their podosomes as rosettes. Hck and Filamin A, which regulate the mesenchymal but not the amoeboid migration mode, also regulate the organization of podosomes as rosettes (Cougoule et al., 2010; Guiet et al., 2012), further supporting the view that these podosome suprastructures are involved in the 3D migration of macrophages in dense matrices (Van Goethem et al., 2011).

In conclusion, this is the first study compiling a detailed analysis of the capacity of human primary blood-derived leukocytes and macrophages to migrate in 3D environments, form podosomes, organize them as rosettes and degrade the ECM. Our results highlight that none of the blood-derived leukocytes studied here do form podosomes or infiltrate a dense matrix of concentrated Matrigel. Thus we suspect that these leukocytes would more likely localize in loose areas of tissues. In addition, our results extend our knowledge on the diversity of macrophage phenotypes by showing that M2 and elicited macrophages use the mesenchymal mode while M1 polarized and resident macrophages do not. Tissues infiltrated by macrophages are often a negative sign of disease progression, including for cancer and chronic inflammation. These diseases are also often characterized by tissue densification (Egeblad et al., 2010) which would likely require the mesenchymal migration. A potential outcome of our work is to consider pathways regulating specifically the mesenchymal migration of macrophages as potential targets for therapeutic approaches.

Acknowledgments

We thank Jean-Michel Sapplayrolles, M. Waqar Aslam and Annie Béhar for technical assistance with macrophage preparations. We thank TRI (Toulouse Réseau Imagerie) and Anexplo GenoToul facilities at the IPBS and Sophie Allard from the IFR150 microscopy platform (Toulouse). We also thank the BiVic facility (Toulouse, France) for the production of lentivirus carrying mCherry-Lifeact construct. This study was supported in part by ARC #2010-120-1733, ANR 2010-01301, FRM DEQ 20110421312. EVG was supported by La Ligue contre le cancer, CL by a Ministère de l'Enseignement Supérieur et de la Recherche fellowships.

Appendix A. Supplementary data

Supplementary data associated with this article can be found, in the online version, at http://dx.doi.org/10.1016/j.ejcb.2012.07.002.

References

Bellingan, G.J., Caldwell, H., Howie, S.E., Dransfield, I., Haslett, C., 1996. In vivo fate of the inflammatory macrophage during the resolution of inflammation: inflammatory macrophages do not die locally, but emigrate to the draining lymph nodes. J. Immunol. 157, 2577–2585.

Ben Amara, A., Ghigo, E., Le Priol, Y., Lepolard, C., Salcedo, S.P., Lemichez, E., Bretelle, F., Capo, C., Mege, J.L., 2010. *Coxiella burnetii*, the agent of Q fever, replicates within trophoblasts and induces a unique transcriptional response. PLoS One 5, e15315.

Bhattacharjee, A., Pal, S., Feldman, G.M., Cathcart, M.K., 2011. Hck is a key regulator of gene expression in alternatively activated human monocytes. J. Biol. Chem. 286, 36709–36723.

Bhuwania, R., Cornfine, S., Fang, Z., Kruger, M., Luna, E.J., Linder, S., 2012. Supervillin couples myosin-dependent contractility to podosomes and enables their turnover. J. Cell Sci. 125, 2300–2314.

Bleul, C.C., Wu, L., Hoxie, J.A., Springer, T.A., Mackay, C.R., 1997. The HIV coreceptors CXCR4 and CCR5 are differentially expressed and regulated on human T lymphocytes. Proc. Natl. Acad. Sci. U.S.A. 94, 1925–1930.

Bystrom, J., Evans, I., Newson, J., Stables, M., Toor, I., van Rooijen, N., Crawford, M., Colville-Nash, P., Farrow, S., Gilroy, D.W., 2008. Resolution-phase macrophages possess a unique inflammatory phenotype that is controlled by cAMP. Blood 112, 4117–4127.

Calle, Y., Anton, I.M., Thrasher, A.J., Jones, G.E., 2008. WASP and WIP regulate podosomes in migrating leukocytes. J. Microsc. 231, 494–505.

Carman, C.V., Sage, P.T., Sciuto, T.E., de la Fuente, M.A., Geha, R.S., Ochs, H.D., Dvorak, H.F., Dvorak, A.M., Springer, T.A., 2007. Transcellular diapedesis is initiated by invasive podosomes. Immunity 26, 784–797.

Cougoule, C., Le Cabec, V., Poincloux, R., Al Saati, T., Mege, J.L., Tabouret, G., Lowell, C.A., Laviolette-Malirat, N., Maridonneau-Parini, I., 2010. Three-dimensional migration of macrophages requires Hck for podosome organization and extracellular matrix proteolysis. Blood 115, 1444–1452.

Davies, L.C., Rosas, M., Smith, P.J., Fraser, D.J., Jones, S.A., Taylor, P.R., 2011. A quantifiable proliferative burst of tissue macrophages restores homeostatic macrophage populations after acute inflammation. Eur. J. Immunol. 41, 2155–2164.

Delavary, B.M., van der Veer, W.M., van Egmond, M., Niessen, F.B., Beelen, R.H., 2011. Macrophages in skin injury and repair. Immunobiology 216, 753–762.

Egeblad, M., Rasch, M.G., Weaver, V.M., 2010. Dynamic interplay between the collagen scaffold and tumor evolution. Curr. Opin. Cell Biol. 22, 697–706.

Fairweather, D., Cihakova, D., 2009. Alternatively activated macrophages in infection and autoimmunity. J. Autoimmun. 33, 222–230.

Fridlender, Z.G., Sun, J., Kim, S., Kapoor, V., Cheng, G., Ling, L., Worthen, G.S., Albelda, S.M., 2009. Polarization of tumor-associated neutrophil phenotype by TGF-beta: "N1" versus "N2" TAN. Cancer Cell 16, 183–194.
Friedl, P., Weigelin, B., 2008. Interstitial leukocyte migration and immune function. Nat. Immunol. 9, 960–969.
Gocheva, V., Wang, H.W., Gadea, B.B., Shree, T., Hunter, K.E., Garfall, A.L., Berman, T., Joyce, J.A., 2010. IL-4 induces cathepsin protease activity in tumor-associated macrophages to promote cancer growth and invasion. Genes Dev. 24, 241–255.
Gordon, S., Mantovani, A., 2011. Diversity and plasticity of mononuclear phagocytes. Eur. J. Immunol. 41, 2470–2472.
Gordon, S., Martinez, F.O., 2010. Alternative activation of macrophages: mechanism and functions. Immunity 32, 593–604.
Guiet, R., Van Goethem, E., Cougoule, C., Balor, S., Valette, A., Al Saati, T., Lowell, C.A., Le Cabec, V., Maridonneau-Parini, I., 2011. The process of macrophage migration promotes matrix metalloproteinase-independent invasion by tumor cells. J. Immunol. 187, 3806–3814.
Guiet, R., Verollet, C., Lamsoul, I., Cougoule, C., Poincloux, R., Labrousse, A., Calderwood, D.A., Glogauer, M., Lutz, P.G., Maridonneau-Parini, I., 2012. Macrophage mesenchymal migration requires podosome stabilization by filamin A. J. Biol. Chem. 287, 13051–13062.
Harunaga, J.S., Yamada, K.M., 2011. Cell-matrix adhesions in 3D. Matrix Biol. 30, 363–368.
Isaac, B.M., Ishihara, D., Nusblat, L.M., Gevrey, J.C., Dovas, A., Condeelis, J., Cox, D., 2010. N-WASP has the ability to compensate for the loss of WASP in macrophage podosome formation and chemotaxis. Exp. Cell Res. 316, 3406–3416.
Jenkins, S.J., Ruckerl, D., Cook, P.C., Jones, L.H., Finkelman, F.D., van Rooijen, N., MacDonald, A.S., Allen, J.E., 2011. Local macrophage proliferation, rather than recruitment from the blood, is a signature of TH2 inflammation. Science 332, 1284–1288.
Krysko, O., Holtappels, G., Zhang, N., Kubica, M., Deswarte, K., Derycke, L., Claeys, S., Hammad, H., Brusselle, G.G., Vandenabeele, P., Krysko, D.V., Bachert, C., 2011. Alternatively activated macrophages and impaired phagocytosis of *S. aureus* in chronic rhinosinusitis. Allergy 66, 396–403.
Larsen, M., Artym, V.V., Green, J.A., Yamada, K.M., 2006. The matrix reorganized: extracellular matrix remodeling and integrin signaling. Curr. Opin. Cell Biol. 18, 463–471.
Laskin, D.L., Sunil, V.R., Gardner, C.R., Laskin, J.D., 2011. Macrophages and tissue injury: agents of defense or destruction? Annu. Rev. Pharmacol. Toxicol. 51, 267–288.
Le Cabec, V., Maridonneau-Parini, I., 1994. Annexin 3 is associated with cytoplasmic granules in neutrophils and monocytes and translocates to the plasma membrane in activated cells. Biochem. J. 303 (Pt 2), 481–487.
Liddiard, K., Rosas, M., Davies, L.C., Jones, S.A., Taylor, P.R., 2011. Macrophage heterogeneity and acute inflammation. Eur. J. Immunol. 41, 2503–2508.
Linder, S., 2007. The matrix corroded: podosomes and invadopodia in extracellular matrix degradation. Trends Cell Biol. 17, 107–117.
Linder, S., Wiesner, C., Himmel, M., 2011. Degrading devices: invadosomes in proteolytic cell invasion. Annu. Rev. Cell Dev. Biol. 27, 185–211.
Mantovani, A., Sica, A., Sozzani, S., Allavena, P., Vecchi, A., Locati, M., 2004. The chemokine system in diverse forms of macrophage activation and polarization. Trends Immunol. 25, 677–686.
Martinez, F.O., Gordon, S., Locati, M., Mantovani, A., 2006. Transcriptional profiling of the human monocyte-to-macrophage differentiation and polarization: new molecules and patterns of gene expression. J. Immunol. 177, 7303–7311.
Martinez, F.O., Helming, L., Gordon, S., 2009. Alternative activation of macrophages: an immunologic functional perspective. Annu. Rev. Immunol. 27, 451–483.
Martinez, F.O., Sica, A., Mantovani, A., Locati, M., 2008. Macrophage activation and polarization. Front. Biosci. 13, 453–461.
Mege, J.L., Mehraj, V., Capo, C., 2011. Macrophage polarization and bacterial infections. Curr. Opin. Infect. Dis. 24, 230–234.
Mosser, D.M., Edwards, J.P., 2008. Exploring the full spectrum of macrophage activation. Nat. Rev. Immunol. 8, 958–969.
Murray, P.J., Wynn, T.A., 2011. Obstacles and opportunities for understanding macrophage polarization. J. Leukoc. Biol. 89, 557–563.
Nourshargh, S., Hordijk, P.L., Sixt, M., 2010. Breaching multiple barriers: leukocyte motility through venular walls and the interstitium. Nat. Rev. Mol. Cell Biol. 11, 366–378.
Qian, B.Z., Pollard, J.W., 2010. Macrophage diversity enhances tumor progression and metastasis. Cell 141, 39–51.
Randolph, G.J., 2008. Emigration of monocyte-derived cells to lymph nodes during resolution of inflammation and its failure in atherosclerosis. Curr. Opin. Lipidol. 19, 462–468.
Ruffell, B., Affara, N.I., Coussens, L.M., 2012. Differential macrophage programming in the tumor microenvironment. Trends Immunol. 33 (3), 119–126.
Sabeh, F., Shimizu-Hirota, R., Weiss, S.J., 2009. Protease-dependent versus - independent cancer cell invasion programs: three-dimensional amoeboid movement revisited. J. Cell Biol. 185, 11–19.
Sage, P.T., Varghese, L.M., Martinelli, R., Sciuto, T.E., Kamei, M., Dvorak, A.M., Springer, T.A., Sharpe, A.H., Carman, C.V., 2012. Antigen recognition is facilitated by invadosome-like protrusions formed by memory/effector T cells. J. Immunol. 188, 3686–3699.
Salmon, H., Franciszkiewicz, K., Damotte, D., Dieu-Nosjean, M.C., Validire, P., Trautmann, A., Mami-Chouaib, F., Donnadieu, E., 2012. Matrix architecture defines the preferential localization and migration of T cells into the stroma of human lung tumors. J. Clin. Invest. 122 (3), 899–910.
Schif-Zuck, S., Gross, N., Assi, S., Rostoker, R., Serhan, C.N., Ariel, A., 2011. Saturated-efferocytosis generates pro-resolving CD11b low macrophages: modulation by resolvins and glucocorticoids. Eur. J. Immunol. 41, 366–379.
Serhan, C.N., Savill, J., 2005. Resolution of inflammation: the beginning programs the end. Nat. Immunol. 6, 1191–1197.
Sica, A., Mantovani, A., 2012. Macrophage plasticity and polarization: in vivo veritas. J. Clin. Invest. 122, 787–795.
Stables, M.J., Shah, S., Camon, E.B., Lovering, R.C., Newson, J., Bystrom, J., Farrow, S., Gilroy, D.W., 2011. Transcriptomic analyses of murine resolution-phase macrophages. Blood 118, e192–e208.
Steadman, R., St John, P.L., Evans, R.A., Thomas, G.J., Davies, M., Heck, L.W., Abrahamson, D.R., 1997. Human neutrophils do not degrade major basement membrane components during chemotactic migration. Int. J. Biochem. Cell Biol. 29, 993–1004.
Szczur, K., Xu, H., Atkinson, S., Zheng, Y., Filippi, M.D., 2006. Rho GTPase CDC42 regulates directionality and random movement via distinct MAPK pathways in neutrophils. Blood 108, 4205–4213.
Tantibhedhyangkul, W., Prachason, T., Waywa, D., El Filali, A., Ghigo, E., Thongnoppakhun, W., Raoult, D., Suputtamongkol, Y., Capo, C., Limwongse, C., Mege, J.L., 2011. Orientia tsutsugamushi stimulates an original gene expression program in monocytes: relationship with gene expression in patients with scrub typhus. PLoS Negl. Trop. Dis. 5, e1028.
Van Goethem, E., Guiet, R., Balor, S., Charriere, G.M., Poincloux, R., Labrousse, A., Maridonneau-Parini, I., Le Cabec, V., 2011. Macrophage podosomes go 3D. Eur. J. Cell Biol. 90, 224–236.
Van Goethem, E., Poincloux, R., Gauffre, F., Maridonneau-Parini, I., Le Cabec, V., 2010. Matrix architecture dictates three-dimensional migration modes of human macrophages: differential involvement of proteases and podosome-like structures. J. Immunol. 184, 1049–1061.
Varin, A., Mukhopadhyay, S., Herbein, G., Gordon, S., 2010. Alternative activation of macrophages by IL-4 impairs phagocytosis of pathogens but potentiates microbial-induced signalling and cytokine secretion. Blood 115, 353–362.
Vereyken, E.J., Heijnen, P.D., Baron, W., de Vries, E.H., Dijkstra, C.D., Teunissen, C.E., 2011. Classically and alternatively activated bone marrow derived macrophages differ in cytoskeletal functions and migration towards specific CNS cell types. J. Neuroinflammation 8, 58.
Verollet, C., Charriere, G.M., Labrousse, A., Cougoule, C., Le Cabec, V., Maridonneau-Parini, I., 2011. Extracellular proteolysis in macrophage migration: losing grip for a breakthrough. Eur. J. Immunol. 41, 2805–2813.
Wolf, K., Friedl, P., 2011. Extracellular matrix determinants of proteolytic and non-proteolytic cell migration. Trends Cell Biol. 21, 736–744.
Wolf, K., Muller, R., Borgmann, S., Brocker, E.B., Friedl, P., 2003. Amoeboid shape change and contact guidance: T-lymphocyte crawling through fibrillar collagen is independent of matrix remodeling by MMPs and other proteases. Blood 102, 3262–3269.